Cumulative shapes of knotted polymers

Eric J. Rawdon[1,*], Kenneth C. Millett[2,**], Vy T. Tran[3,***], and Andrzej Stasiak[4,†]

[1] *Department of Mathematics, University of St. Thomas, Saint Paul, MN 55105, USA*
[2] *Department of Mathematics, University of California, Santa Barbara, CA 93106, USA*
[3] *Department of Physics, Washington University, Saint Louis, MO 63130, USA*
[4] *Center for Integrative Genomics, Faculty of Biology and Medicine, University of Lausanne, CH 1015, Switzerland*

We investigate the influence of knotting and chirality on the shape of knotted polygons forming trefoil knots compared to unknotted polygons by aligning independent configurations along their principal inertial axes. While for six edge polygons forming trefoil knots the chiral knotted structure is revealed in the isodensity profiles, the distinct chiral signature of the trefoil is significantly diminished with 24 edges. We observe that as the number of edges in the polygons increases, the cumulative shapes of trefoil knots progressively approach the cumulative shapes for unknotted polygons.

§1. Introduction

To understand the influence of a polymer's topology on its overall shape, we characterize the cumulative shapes resulting from aligning individual realizations of random polygons with different chain sizes and topologies. Inspired by the work of Theodorou and Suter,[19] who considered the mass density distributions of linear polymer chains aligned with respect to their three principal axes of inertia in order of decreasing moment, we have extended their method by proposing a symmetry breaking algorithm as a strategy to detect the impact of knotting and chirality present in polymer chains.[12]

Employing the model of freely moving polymers in solution, i.e. freely jointed equilateral open and closed chains, we previously have investigated[12] the consequences of knotting in very short chains, having only six bonds, as this is the first length in which non-trivial knotting can occur. Here, we investigate the evolution of the cumulative average sizes and shapes of knotted polymers as the number of bonds in the polymer increases.

---

*) Email: ejrawdon@stthomas.edu
**) Email: millett@math.ucsb.edu
***) Email: vytran@wustl.edu
†) Email: andrzej.stasiak@unil.ch

§2. Data Generation

Our goal is to analyze the effect of topology, chirality, and length on vertex isodensity surfaces for random polygons in three-dimensional Euclidean space. We analyzed three topological knot types (unknots, left-handed trefoils (data not shown), and right-handed trefoils) at three different polymer lengths (6, 24, and 50 edges). Polygons were generated using a modified Hedgehog algorithm.[7),14)]

For completeness sake, we describe our modified Hedgehog algorithm. To construct one n-edge polygon (where n is even), we generate a list of $n/2$ random vectors on the unit sphere. We add the $n/2$ opposite vectors to the list, which gives us a set of n vectors whose sum is the **0**-vector. We then perform a series of moves to break the self-correlations between vectors in the list. A random integer k between 2 and $n/2$ is generated and k vectors are chosen randomly from our list. We perform a random rotation of size $0 \leq \theta < 2\pi$ to the k vectors about the axis determined by the sum of the k vectors. This leaves the sum of the k vectors constant, and thus the sum of all n vectors remains the **0**-vector. We perform $10n^2$ of these randomizing moves for each set of n vectors.

The knot types of the configurations are determined using the HOMFLYPT polynomial code of Ewing and Millett.[2)] The HOMFLYPT polynomial[3),15)] is not a perfect representation of knot type, i.e. there are different knot types that have the same HOMFLYPT polynomial. However, to date there are no known non-trivial knot types with the same HOMFLYPT polynomial as the unknot nor knot types with the same HOMFLYPT polynomial as the trefoil knot. Thus, we expect no contamination in the range of edges that we analyze.

For 6 edge polymers, we analyzed 199,977 unknots, 92,309 right-handed trefoils, and 92,330 left-handed trefoils (these configurations were also analyzed in Ref. 12)). For 24 edge polymers, we analyzed 369,286 unknots, 36,510 right-handed trefoils, and 36,432 left-handed trefoils. For 50 edge polymers, we analyzed 258,219 unknots, 39,012 right-handed trefoils, and 39,172 left-handed trefoils.

The configurations are then rigidly translated and rotated into a standard position as follows. For the Theodorou and Suter (TS) alignment[19)] on a given polygon, we first compute the center of mass of the polygon (assuming that the mass of the polygon is equally distributed over its vertices) and translate the polygon so that the center of mass coincides with the origin. Next we compute the gyration tensor for the (now translated) polygon. The eigenvectors of the gyration tensor are the principal axes of rotation of the polygon and determine a mutually orthogonal system of three vectors. The polygon is then rotated so that the eigenvector associated with the largest eigenvalue coincides with the x-axis and the eigenvector associated with the second largest eigenvalue coincides with the y-axis. Note that the third eigenvector naturally coincides with the z-axis. This ends the TS alignment procedure.

Eigenvectors are inherently non-oriented, i.e. there is no natural positive and negative direction for the eigenvector. As a result, the TS alignment generates surfaces with 180° rotational symmetry. However, individual configurations are generically not symmetric.[5)] To distinguish this asymmetry, we defined a new alignment in Ref. 12) called the *Symmetry Breaking Algorithm (SBA)*. The first steps of the al-

gorithm are identical to the TS alignment procedure, first translate the knot so that the center of mass is at the origin and then compute the eigenvectors and eigenvalues of the gyration tensor. Our goal is to define a default orientation for the system of vectors defining the principal axes for each polygon. We choose the orientation for the x-axis to be so that the largest x-coordinate of the polymer vertices lies in positive x-direction. We then choose the orientation for the y-axis to be so that the largest y-coordinate lies in the positive y-direction. Note that the z-axis is fixed based on the choices of x- and y-axes.

Once we have aligned a group of polymer configurations, we generate a smoothed 3D histogram of the data as follows:

1. Determine the extreme values in the x, y, and z directions;
2. Calculate the average density, d, of the points, assuming they are distributed throughout an ellipsoid with axes corresponding to the range in each direction;
3. Calculate the mean free distance, $m = (1/d)^{1/3}$, which gives a rough estimate of the average distance between a point and its nearest neighbor;
4. Create an array of voxels with side length $8m/3$;
5. Read in each point in the data set one at a time, center a 3D Gaussian with standard deviation $2m$ at the point;
6. For each voxel in the $7 \times 7 \times 7$ region of voxels surrounding the point, integrate the Gaussian inside the voxel and add that amount to the voxel value.

A point density function then is computed using a cubic spline interpolation. To compute the isodensity surfaces, we let ρ_{max} be the maximum density of the point density function. Then for a given density value ρ, given as a percentage of ρ_{max}, the isodensity surface is a level curve of the point density function.

§3. Results

Both the TS and SBA methods visibly distinguish the unknotted and knotted conformations in the case of six-edge polygons, see the top rows of Figs. 1 and 2 (TS method) and Figs. 3 and 4 (SBA method). The six-edge trefoil knots are significantly more compact than the unknots and the internal structure of their cumulative shape surfaces differs significantly from that of the unknots. For 24 and 50 edges (the bottom two rows of the figures), however, these differences are much less visible for both the TS and SBA methods. Indeed, the shapes of the isodensity surfaces obtained by a given method appear to be nearly the same for knots and unknots although they differ in scale.

To quantify the difference in scale, we show the linear span of the extreme vertex points in the directions of the three principal axes of rotation in Table I (for the TS method) and in Table II (for the SBA method). In Table III, we show the ratio of the right-handed trefoil span to the unknot span for the two methods. These ratios appear to be converging to one as the length of the polymers increase, demonstrating the decreasing influence of the presence of the trefoil knot and its associated chirality as the number of edges in the analyzed polygons increases.

We note that the evolution of the overall shapes of the unknotted and knotted polygons as their chain length increases is consistent with a high degree of knot local-

Table I. The linear dimensions (spans) along the three principal axes of rotation of the cumulative shapes of unknotted and right-handed trefoil knotted polygons aligned using the TS method.

TS	Unknots			Right-handed trefoils		
Edges	x	y	z	x	y	z
6	2.96	2.24	1.52	1.91	1.60	1.33
24	8.39	6.08	4.21	7.45	5.32	3.73
50	12.98	9.37	6.50	11.89	8.50	6.22

Table II. The linear dimensions (spans) along the three principal axes of rotation of the cumulative shapes of unknotted and right-handed trefoil knotted polygons aligned using the SBA method.

SBA	Unknots			Right-handed trefoils		
Edges	x	y	z	x	y	z
6	2.95	2.11	1.52	1.88	1.47	1.33
24	8.19	5.80	4.26	7.03	4.82	3.74
50	12.16	8.82	6.62	11.32	7.86	6.40

Table III. The trefoil/unknot ratio of spans along the three principal axes of rotation.

	TS			SBA		
Edges	x	y	z	x	y	z
6	0.65	0.72	0.87	0.64	0.70	0.87
24	0.89	0.87	0.89	0.86	0.83	0.88
50	0.92	0.91	0.96	0.93	0.89	0.97

ization.[1),4),6),9),10)] This appears to play an essential role in the average structure of polymer chains, even at relatively small length scales. While, for larger polygons, the isodensity surfaces resemble the "bar of soap" structure identified in the Theodorou-Suter, the SBA surfaces adopt a shape similar to a bean. Such a shape was predicted as a cumulative shape of random walks provided that the intrinsic asymmetry of individual configurations is utilized for their alignment.[8)]

§4. Conclusions

While the presence of chirality is visible in the isodensity surface structure for hexagonal trefoil knots, its signature quickly vanishes as the presence of chirally knotted regions becomes diluted by the presence of much larger achiral unknotted regions of the polymer chains constituting an increasingly large proportion of the polymer chains. The overall average cumulative sizes of trefoil knots and unknots become closer as the number of bonds increases. While their shapes appear, visually, to become similar as the number of bonds increases, this facet of our study would require further investigation to confirm this conjecture. A somewhat similar evolution of the sizes and shapes of unknots and knots with increasing chain size was observed
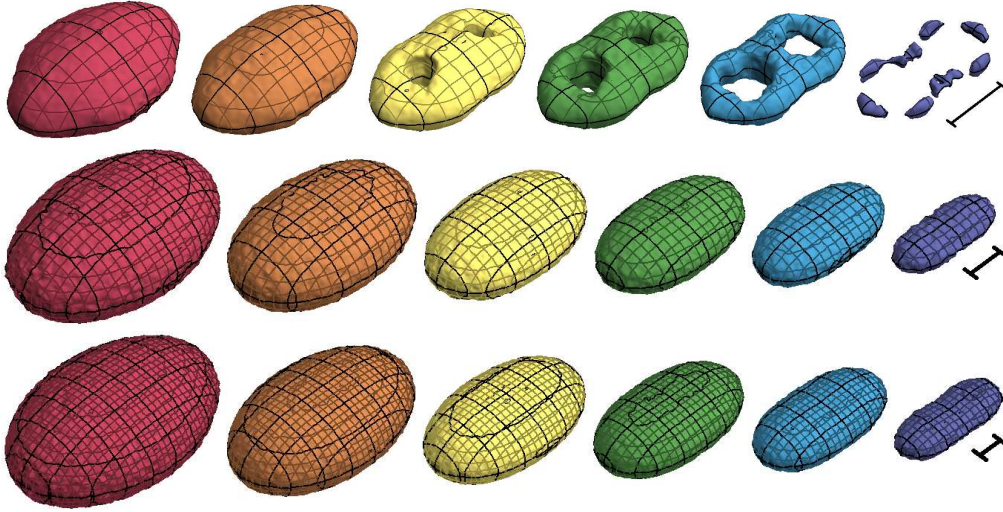
Fig. 1.   The cumulative shapes of unknotted random polygons that were aligned using the TS method. The shapes are presented as series of isodensity surfaces with increasing density of occupation. The leftmost surfaces have a low density of occupation and enclose ca. 95% of all vertices contributing to a superimposed set of co-aligned configurations, while the rightmost surfaces are these with high density of occupation but enclose only ca. 10% of all contributing vertices. The shown isodensity surfaces have voxels densities of $0.03\rho_{max}$, $0.10\rho_{max}$, $0.25\rho_{max}$, $0.35\rho_{max}$, $0.5\rho_{max}$, and $0.75\rho_{max}$, respectively, where ρ_{max} is the maximum voxel density within a given class of polygons and a given method of alignment. The sequential rows correspond to polygons with 6, 24 and 50 segments, respectively. The scale bars in the respective rows correspond to one segment length.
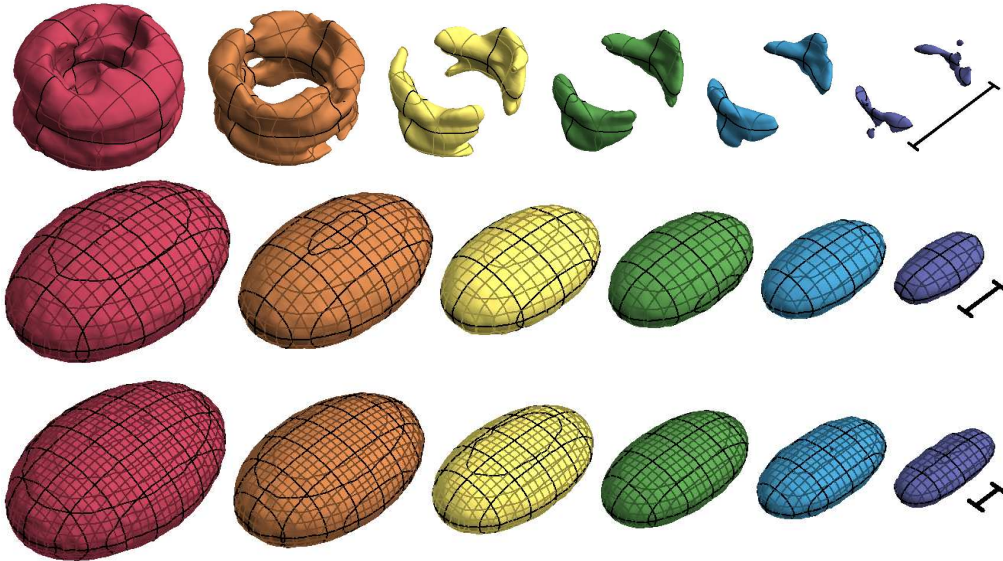
Fig. 2.   The cumulative shapes of random polygons forming right-handed trefoil knots that were aligned using the TS method. See the legend to Fig. 1 for an explanation of the elements of the figure.
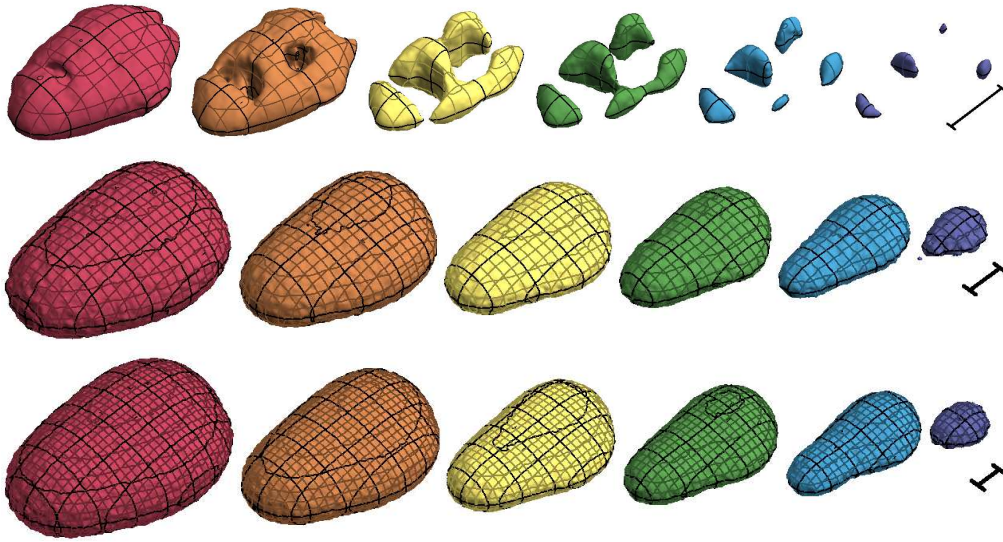
Fig. 3. The cumulative shapes of unknotted random polygons that were aligned using the SBA method. See the legend to Fig. 1 for an explanation of the elements of the figure.
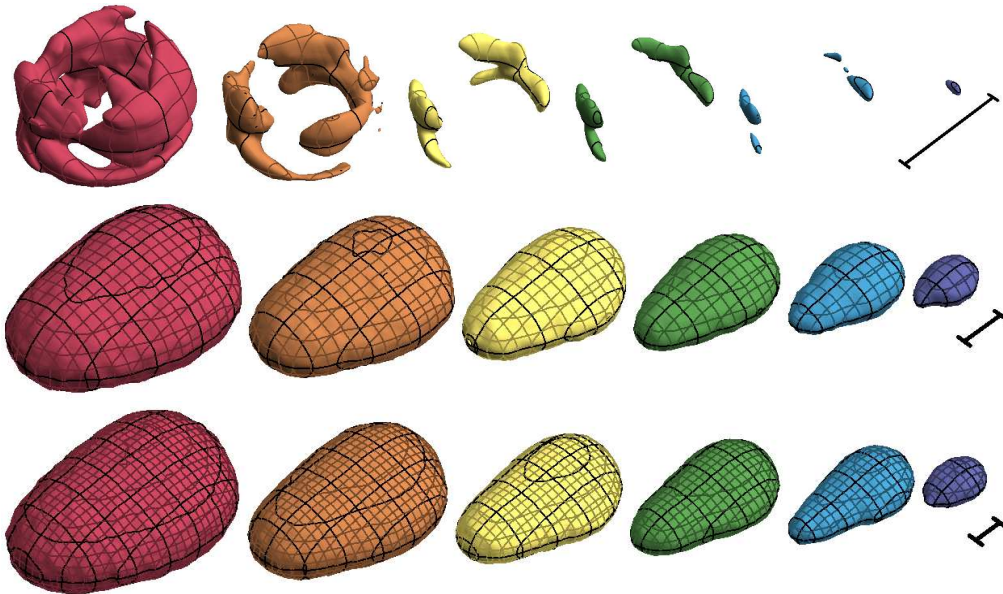
Fig. 4. The cumulative shapes of random polygons forming right-handed trefoil knots that were aligned using the SBA method. See the legend to Fig. 1 for an explanation of the elements of the figure.

for such measures as the radius of gyration[13), 17), 18)] and the asphericity (a measure of shape) and axial dimensions of ellipsoids of inertia[16)] and enveloping ellipsoids.[11)]

Acknowledgments

References

1) E. Ercolini, F. Valle, J. Adamcik, G. Witz, R. Metzler, P. De Los Rios, J. Roca, and G. Dietler, Phys. Rev. Lett. **98** (2007), 058102.
2) B. Ewing and K. C. Millett, In *Progress in knot theory and related topics* (1997), 51.
3) P. Freyd, D. Yetter, J. Hoste, W. B. R. Lickorish, K. Millett, and A. Ocneanu, Bull. Amer. Math. Soc. **12** (1985), 239.
4) E. Guitter and E. Orlandini, J. Phys. A **32** (1999), 1359.
5) C. Haber, S. A. Ruiz, and D. Wirtz, Proc. Natl. Acad. Sci. USA **97** (2000), 10792.
6) V. Katritch, W. K. Olson, A. Vologodskii, J. Dubochet, and A. Stasiak, Phys. Rev. E **61** (2000), 5545.
7) K. V. Klenin, A. V. Vologodskii, V. V. Anshelevich, A. M. Dykhne, and M. D. Frank-Kamenetskii, J. Biomol. Struct. Dyn. **5** (1988), 1173.
8) W. Kuhn, Kolloid-Z. **68** (1934), 2.
9) M. L. Mansfield and J. F. Douglas, J. Chem. Phys. **133** (2010), 044903.
10) B. Marcone, E. Orlandini, A. L. Stella, and F. Zonta, Phys. Rev. E **75** (2007), 041105.
11) K. C. Millett, P. Plunkett, M. Piatek, E. J. Rawdon, and A. Stasiak, J. Chem. Phys. **130** (2009), 165104.
12) K. C. Millett, E. J. Rawdon, V. T. Tran, and A. Stasiak, J. Chem. Phys. **133** (2010), 154113.
13) E. Orlandini, M. C. Tesi, E. J. Janse van Rensburg, and S. G. Whittington, J. Phys. A **31** (1998), 5953.
14) P. Plunkett, M. Piatek, A. Dobay, J. C. Kern, K. C. Millett, A. Stasiak, and E. J. Rawdon, Macromolecules **40** (2007), 3860.
15) J. H. Przytycki and P. Traczyk, Kobe J. Math. **4** (1987), 115.
16) E. J. Rawdon, J. C. Kern, M. Piatek, P. Plunkett, A. Stasiak, and K. C. Millett, Macromolecules **41** (2008), 8281.
17) M. K. Shimamura and T. Deguchi, Phys. Rev. E **65** (2002), 051802.
18) M. K. Shimamura and T. Deguchi. In *Physical and numerical models in knot theory* (2005), 399.
19) D. N. Theodorou and U. W. Suter. Macromolecules **18** (1985), 1206.